Increased x-ray attenuation in malignant vs. benign mediastinal nodes in an orthotopic model of lung cancer

Paul Flechsig
Peter Choyke
Clemens Kratochwil
Arne Warth
Gerald Antoch
Tim Holland-Letz
Daniel Rath
Viktoria Eichwald
Peter E. Huber
Hans-Ulrich Kauczor
Uwe Haberkorn
Frederik L. Giesel

PURPOSE
Staging of lung cancer is typically performed with fluorodeoxyglucose-positron emission tomography-computed tomography (FDG-PET/CT); however, false positive PET scans can occur due to inflammatory disease. The CT scan is used for anatomic registration and attenuation correction. Herein, we evaluated x-ray attenuation (XRA) within nodes on CT and correlated this with the presence of malignancy in an orthotopic lung cancer model in rats.

METHODS
1×10^6 NCI-H460 cells were injected transthoracically in six National Institutes of Health nude rats and six animals served as controls. After two weeks, animals were sacrificed; lymph nodes were extracted and scanned with a micro-CT to determine their XRA prior to histologic analysis.

RESULTS
Median CT density in malignant lymph nodes (n=20) was significantly higher than benign lymph nodes (n=12; $P = 0.018$). Short-axis diameter of metastatic lymph nodes was significantly different than benign nodes (3.4 mm vs. 2.4 mm; $P = 0.025$). Area under the curve for malignancy was higher for density-based lymph node analysis compared with size measurements (0.87 vs. 0.7).

CONCLUSION
XRA of metastatic mediastinal lymph nodes is significantly higher than benign nodes in this lung cancer model. This suggests that information on nodal density may be useful when used in combination with the results of FDG-PET in determining the likelihood of malignant adenopathy.

From the Departments of Diagnostic and Interventional Radiology (P.F., H.U.K.), Nuclear Medicine (C.K., D.R., U.H., ✉ *frederik@egiesel.com*), Institute of Pathology (A.W.), University Hospital Heidelberg, Heidelberg, Germany; Molecular Imaging Program (P.C.), Center for Cancer Research, National Cancer Institute, Bethesda, Maryland, USA; the Department of Diagnostic and Interventional Radiology (G.A.), University Dusseldorf, School of Medicine, Düsseldorf, Germany; Core Facility of Statistics (T.H.L.) and Core Facility Small Animal Imaging (V.E.), German Cancer Research Center, Heidelberg, Germany; Molecular Radiation Oncology (P.E.H.), German Cancer Research Center and University Hospital Center Heidelberg, Heidelberg, Germany; Translational Lung Research Center Heidelberg (H.U.K., F.L.G.), Member of the German Center for Lung Research DZL; Heidelberg, Germany.

Lung cancer is the leading cause of cancer deaths in the United States and Europe (1). Choice of therapy and prognosis is determined by the stage at which lung cancer is detected. Mediastinal nodal involvement is a significant negative prognostic sign and portends a shorter time to progression (2). Fluorodeoxyglucose-positron emission tomography-computed tomography (FDG-PET/CT) has emerged as the leading noninvasive staging method as both primary tumor and mediastinal nodes can be assessed (2, 3). Precise mediastinal N-staging is mandatory since patients with contralateral or multiregional mediastinal lymph node metastases are often excluded from primary surgery (4). The PET component of the FDG-PET/CT examination is typically assessed by measuring the maximum standardized uptake value (SUV_{max}) in the primary tumor and nodes. However, the FDG-PET component is sometimes equivocal due to false positive uptake in inflammatory nodes (5). The CT component is typically assessed using Response Evaluation Criteria In Solid Tumors (RECIST 1.1) criteria in the primary and nodes, and it is based on the node's short-axis diameter (3). However, size changes are notoriously unreliable in assessing disease status. Therefore, staging often requires additional invasive methods such as transbronchial biopsy or mediastinoscopy for histologic verification (6), especially in patients that might benefit from primary surgery.

Previous reports have suggested that nodes exhibit increases in x-ray attenuation (XRA) density when they become malignant due to replacement of the fatty nodal hilum with cancer cells (5). For instance, malignant lymph nodes obtained from patients with breast cancer showed increased density on grating-based phase-contrast x-ray tomography (7–10). However, this observation is not routinely incorporated into clinical interpretation of PET/CT despite the ready availability of such information. In order to further investigate potential density changes in metastatic and nonmetastatic mediastinal and hilar lymph nodes, we utilized an

orthotopic lung cancer model in nude rats (11), which included *ex vivo* micro-CT XRA of extracted lymph nodes two weeks after transthoracic tumor cell implantation (Fig. 1). Findings were correlated with histology.

Methods

### Animal treatment, reagents, and study design

A total of 12 male nude rats (CR:NIH-RNU), including six animals as controls, aged four weeks were acclimatized for two weeks prior to tumor implantation. Animals were housed in sterilized cages, fed autoclaved food and water ad libitum and were assessed daily for signs of distress in compliance with international standards of humane treatment of animals in research. The study was approved by the local responsible authorities and conducted according to the guidelines of the institutional review board, the Declaration of Helsinki, and the NIH guidelines for use of laboratory animals.

A total of 1×10^6 NCI-H460 cells were mixed 1:1 with matrigel in a final volume of 50 μL (11, 12). Prior to implantation, animals were anesthetized using Isoflurane. Cells were transthoracically injected in the fifth intercostal space using a 28G ½″ needle (12).

Two weeks after injection, animals were sacrificed and lymph nodes were extracted. Directly after extraction, lymph nodes were examined in a micro-CT (Siemens Inveon) and thereafter placed in formalin and stained with hematoxylin and eosin (HE) for histologic analysis (Fig. 2).

Ex vivo micro-CT

CT scanning was performed using a micro-CT scanner (Siemens Inveon MultiMo-
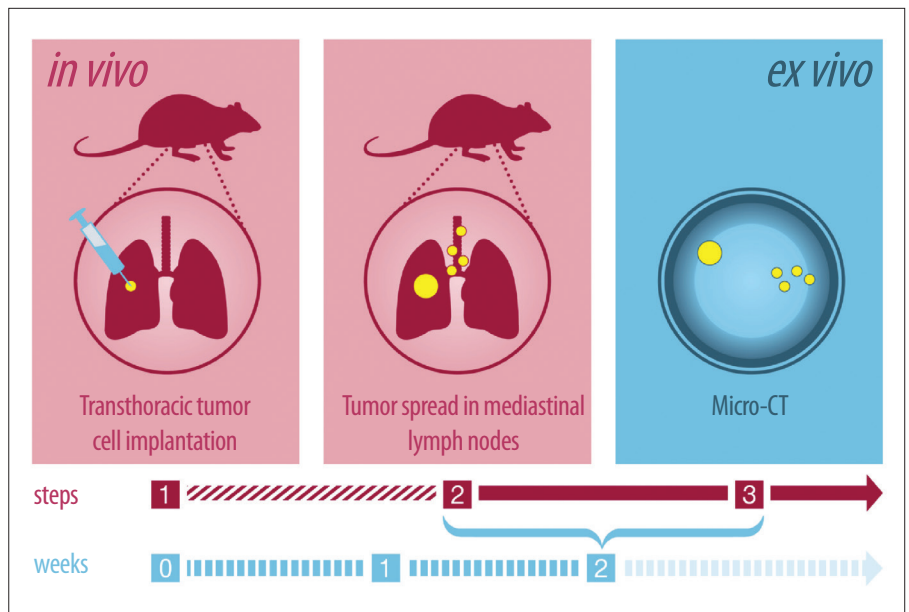
Figure 1. Study design with *in vivo* and *ex vivo* measurements. Step 1: Transthoracic tumor cell transplantation in the 5th intercostal space. Step 2: Within the first two weeks after transthoracic tumor cell transplantation tumor spreads in mediastinal and hilar lymph nodes *(small yellow dots)*. Primary tumor is seen in the right lower lobe *(big yellow dot)*. Step 3: Micro-CT examination of extracted mediastinal lymph nodes.

dality). The scanning parameters were set to 60 kV, 500 μA, 400 ms exposure time, 360° rotation with 360 rotation steps, field of view 48.64×56.25 mm and binning factor 2. Under low-medium magnification the effective pixel size was 47.5 μm. CT images were reconstructed with a down sample factor of 2 using Cobra Reconstruction Software.

Postprocessing

For computing the XRA histograms, lymph nodes were segmented by a radiologist who was blinded with regard to whether the nodes came from an experimental animal or a control, using a semi-automatic method (Fraunhofer MEVIS). Semi-automated lymph node XRA histograms were obtained by identifying a seed point in the middle of each lymph node. The semi-automated segmentation generated density thresholds that identified the contours of the node. If necessary, segmentation results were corrected manually in all three dimensions. Imaging findings were correlated to histology.

Statistical analysis

Density and short-axis diameter data were summarized using descriptive statistics (mean, standard deviation [SD], median, minimum, and maximum) and illustrated in Box-Whisker-Plots (Fig. 3). Differences were considered significant

at $P < 0.05$ in a two-sided unpaired *t* test. As multiple, possibly correlated lymph nodes were investigated per animal, average densities and short-axis diameters were calculated for each animal, and only these averages were used as experimental units for the t-tests.

Diagnostic properties of the parameters were investigated in a Receiver Operating Characteristic (ROC) analysis. The optimal cutoff value was defined as the cutoff maximizing the sum of sensitivity and specificity (Youden index) in detection of malignant lymph nodes.

Statistical analysis was performed using SigmaPlot (Systat Software GmbH).
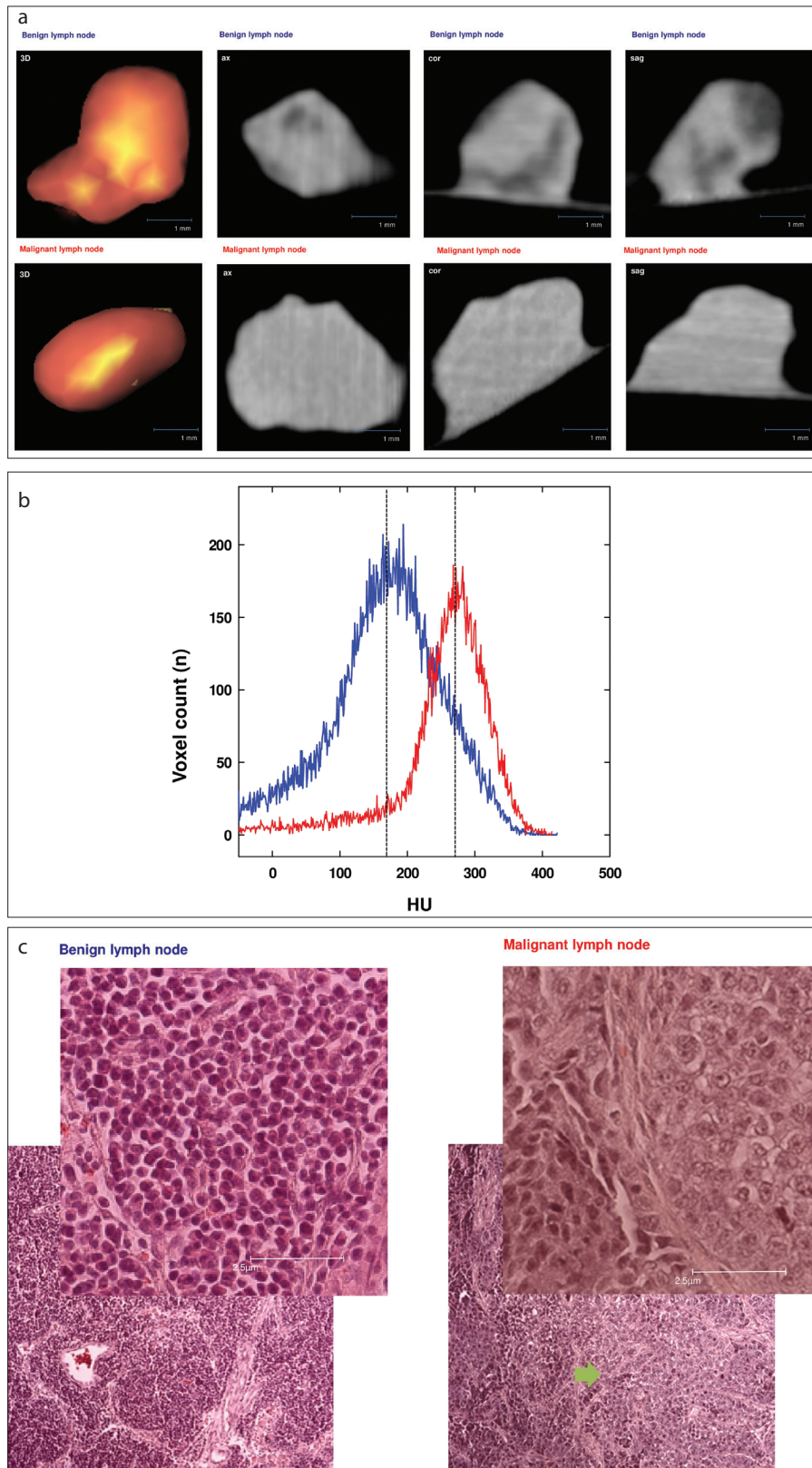
Results

All removed nodes were analyzed with *ex vivo* micro-CT (Fig. 2). A total number of 20 malignant lymph nodes demonstrated a median CT density of 125.9 Hounsfield Units (HU) (mean±SD, 127.8±64.5 HU; Fig. 3a). Histologically negative lymph nodes (n=12) resected from the control group, demonstrated a median CT density of 13.9 HU (mean±SD, 12.6±86.1 HU; Fig. 3a). Comparison of mean CT densities between affected and unaffected lymph nodes was statistically significant ($P = 0.018$).

The best possible cutoff value for the discrimination between malignant and benign

Figure 2. a–c. Correlation of micro-CT **(a)**, histogram **(b)**, and histopathologic cross-section **(c)**. Examples of benign *(blue)* and malignant *(red)* lymph node histology are shown. Panel **(a)** shows micro-CT with 3D reconstruction, in axial, coronary, and sagittal views. Panel **(b)** shows exemplary extracts of histograms: left histogram represents a benign lymph node *(blue line)*, right histogram represents a malignant lymph node *(red line)* with median densities indicated by dotted vertical lines (HU, Hounsfield unit). Panel **(c)** shows corresponding histologic HE-stained cross-sections (foreground in right upper corner: 40× magnification; background: 10× magnification). The left column in panel **(c)** shows physiologic lymph node structures (benign), while the right column shows rat lymph node with irregular lymph node tissue and infiltrates of a solid carcinoma *(arrow)*.

lymph nodes was 68.8 HU with 17 out of 20 malignant lymph nodes having a density above 68.8 HU (85%) and 10 out of 12 benign lymph nodes measuring below 68.8 HU (83%, Fig. 3b).

Histologically proven metastatic lymph nodes had a slightly higher short-axis diameter compared with histologically negative ones. Specifically, metastatic lymph nodes demonstrated a median short-axis diameter of 3.35 mm (mean±SD, 4.2±2.0 mm; Fig. 3c), while negative nodes demonstrated a median short-axis diameter of 2.35 mm (mean±SD, 2.8±1.7 mm; $P = 0.025$ accounting for multiple nodes per rat; Fig. 3c).

ROC analysis revealed an area under the curve (AUC) for malignancy of 0.7 for short-axis diameter and 0.87 for density changes (Fig. 3d).

Discussion

This study shows that malignant nodes have significantly higher XRA than benign nodes in an orthotopic lung cancer model in nude rats. Density differences between malignant and benign lymph nodes were more predictive of metastatic involvement than the short-axis diameter, which was reflected in a higher diagnostic AUC (87%) for density changes than for short-axis diameter (70%).

Several previous studies have suggested a correlation between XRA and node status. For instance, Tapfer et al. (7) and Momose et al. (9) used grating-based phase-contrast x-ray tomography, and demonstrated high specificity, sensitivity, and positive and negative predictive values for this methodology (10). Jensen et al. (10) reported the visibility of lymphoid follicles in nonmetastatic lymph nodes, whereas metastatic lesions had lost their ordered morphology and had higher XRA. Even though we could not detect internal structures within lymph nodes with micro-CT, we detected statistically significant increase in lymph node XRA density, which correlated with malignant histology.

This work suggests that CT density measurements may play a role in increasing or decreasing the risk assessment for malignant nodal involvement based on FDG-PET/CT. Accurate assessment of lymph node status is crucial for therapeutic planning and prognosis (13–19). Currently, PET uptake is measured by SUV$_{max}$ values, while the CT-component utilizes RECIST 1.1 short axis linear measurements (20, 21). Our findings
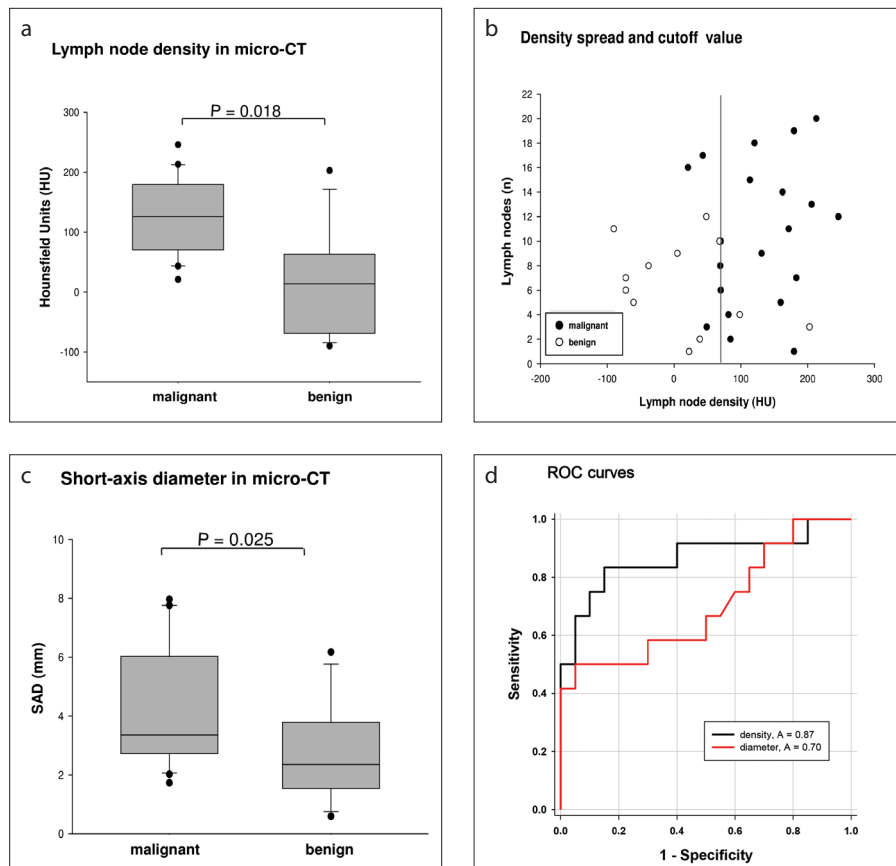
Figure 3. a–d. Statistical evaluation of micro-CT measurements of resected lymph nodes. Panel **(a)** shows density of lymph nodes in micro-CT. CT density measurements of metastatic and benign lymph nodes were significantly different. Median CT density is 125.9 HU for malignant lymph nodes and 13.9 HU for benign lymph nodes (*P* = 0.018). Panel **(b)** shows density spread of resected lymph nodes with a possible cutoff value (68.6 HU). Panel **(c)** shows short-axis diameter (SAD) of lymph nodes: metastatic lymph nodes demonstrate higher short-axis diameter compared with benign lymph nodes (3.35 mm vs. 2.35 mm, *P* = 0.025). Panel **(d)** shows ROC curves with AUC for lymph node density and short-axis diameter.

suggest that lymph node density may also provide useful diagnostic information, potentially within time-saving semi-automatic measurements (22). It is also possible that dual energy CT may enable even better discrimination of XRA than single energy CT performed in our experiment (23), and that dual energy CT could give further information on nodal status based on the measurement of iodine uptake in contrast-enhanced dual-phase dual-energy CT (24).

This work has several important limitations. Only a relatively small number (n=32) of histologically proven lymph nodes were investigated on only 12 animals. Normal nodes in rats are very difficult to identify due to their small size. Moreover, the study was only conducted in one species using one tumor model, which might not be applicable to most human tumors. Certainly the density difference between positive and negative nodes in this study is higher than would be expected in patients. To what extent this is influenced by performing these measurements *ex vivo* on a micro-CT unit is also unknown. Therefore, future work in this field should focus on prospective trials of CT nodal density measurements in large patient cohorts. Such large numbers of subjects could permit the identification of reasonable threshold values of density that result in clinically relevant increases in the detection of malignant nodes. This might be especially helpful in cases of FDG-equivocal lymph nodes and might therefore be of substantial importance for a better exploitation of hybrid imaging in daily routine. By adding the parameter of CT density to lymph node dimensions and FDG-PET/CT activity, more accurate characterization of node status, with fewer false positives could be achieved, thus sparing patients from unnecessary interventions prior to therapy.

In conclusion, density measurement of indeterminate lymph nodes seems to be a promising and potentially clinically valuable imaging parameter that might improve noninvasive lung cancer staging. By means of density measurements one could possibly make better use of FDG-PET/CT in order to improve therapy stratifications prior to therapy.

Conflict of interest disclosure
The authors declared no conflicts of interest.

References
1. Rivera MP. Lung cancer in women: differences in epidemiology, biology, histology, and treatment outcomes. Semin Respir Crit Care Med 2013; 34:792–801. [CrossRef]
2. Abramyuk A, Appold S, Zophel K, Hietschold V, Baumann M, Abolmaali N. Quantitative modifications of TNM staging, clinical staging and therapeutic intent by FDG-PET/CT in patients with non-small cell lung cancer scheduled for radiotherapy--a retrospective study. Lung Cancer 2012; 78:148–152. [CrossRef]
3. Kratochwil C, Haberkorn U, Giesel FL. PET/CT for diagnostics and therapy stratification of lung cancer. Radiologe 2010; 50:684–691. [CrossRef]
4. Rami-Porta R, Call S. Invasive staging of mediastinal lymph nodes: mediastinoscopy and remediastinoscopy. Thorac Surg Clin 2012; 22:177–189. [CrossRef]
5. Flechsig P, Kratochwil C, Schwartz LH, et al. Quantitative volumetric CT-histogram analysis in N-staging of 18F-FDG-equivocal patients with lung cancer. J Nucl Med 2014; 55:559–564. [CrossRef]
6. Goeckenjan G, Sitter H, Thomas M, et al. Prevention, diagnosis, therapy, and follow-up of lung cancer: interdisciplinary guideline of the German Respiratory Society and the German Cancer Society. Pneumologie 2011; 65:39–59. [CrossRef]
7. Tapfer A, Bech M, Velroyen A, et al. Experimental results from a preclinical X-ray phase-contrast CT scanner. Proc Natl Acad Sci USA 2012;109:15691–15696. [CrossRef]
8. Pfeiffer F, Bunk O, David C, et al. High-resolution brain tumor visualization using three-dimensional x-ray phase contrast tomography. Phys Med Biol 2007; 52:6923–6930. [CrossRef]
9. Momose A, Yashiro W, Harasse S, Kuwabara H. Four-dimensional X-ray phase tomography with Talbot interferometry and white synchrotron radiation: dynamic observation of a living worm. Opt Express 2011; 19:8423–8432. [CrossRef]
10. Jensen TH, Bech M, Binderup T, et al. Imaging of metastatic lymph nodes by X-ray phase-contrast micro-tomography. PloS One 2013; 8:e54047. [CrossRef]
11. Liu J, Blackhall F, Seiden-Long I, et al. Modeling of lung cancer by an orthotopically growing H460SM variant cell line reveals novel candidate genes for systemic metastasis. Oncogene 2004; 23:6316–6324. [CrossRef]
12. Saha D, Watkins L, Yin Y, et al. An orthotopic lung tumor model for image-guided microirradiation in rats. J Radiat Res 2010; 174:62–71. [CrossRef]

13. Toloza EM, Harpole L, McCrory DC. Noninvasive staging of non-small cell lung cancer: a review of the current evidence. Chest 2003; 123(Suppl 1):137S–146S. **[CrossRef]**

14. Birim O, Kappetein AP, Stijnen T, Bogers AJ. Meta-analysis of positron emission tomographic and computed tomographic imaging in detecting mediastinal lymph node metastases in nonsmall cell lung cancer. Ann Thorac Surg 2005; 79:375–382. **[CrossRef]**

15. Schaefer NG, Hany TF, Taverna C, et al. Non-Hodgkin lymphoma and Hodgkin disease: coregistered FDG PET and CT at staging and restaging--do we need contrast-enhanced CT? Radiology 2004; 232:823–829. **[CrossRef]**

16. Gould MK, Kuschner WG, Rydzak CE, et al. Test performance of positron emission tomography and computed tomography for mediastinal staging in patients with non-small-cell lung cancer: a meta-analysis. Ann Intern Med 2003; 139:879–892. **[CrossRef]**

17. Hellwig D, Baum RP, Kirsch C. FDG-PET, PET/CT and conventional nuclear medicine procedures in the evaluation of lung cancer: a systematic review. Nuklearmedizin 2009; 48:59–69. **[CrossRef]**

18. Silvestri GA, Gould MK, Margolis ML, et al. Non-invasive staging of non-small cell lung cancer: ACCP evidenced-based clinical practice guidelines (2nd edition). Chest 2007; 132(Suppl 3):178S–201S.

19. Beyer F, Buerke B, Gerss J, et al. Prediction of lymph node metastases in NSCLC. Three dimensional anatomical parameters do not substitute FDG-PET-CT. Nuklearmedizin 2010; 49:41–48.

20. Eisenhauer EA, Therasse P, Bogaerts J, et al. New response evaluation criteria in solid tumours: revised RECIST guideline (version 1.1). Eur J Cancer 2009; 45:228–247. **[CrossRef]**

21. Tournoy KG, Maddens S, Gosselin R, Van Maele G, van Meerbeeck JP, Kelles A. Integrated FDG-PET/CT does not make invasive staging of the intrathoracic lymph nodes in non-small cell lung cancer redundant: a prospective study. Thorax 2007; 62:696–701. **[CrossRef]**

22. Hoink AJ, Wessling J, Koch R, et al. Comparison of manual and semi-automatic measuring techniques in MSCT scans of patients with lymphoma: a multicentre study. Eur Radiol 2014; 24:2709–2718. **[CrossRef]**

23. Zachrisson H, Engstrom E, Engvall J, Wigstrom L, Smedby O, Persson A. Soft tissue discrimination ex vivo by dual energy computed tomography. Eur J Radiol 2010;75:e124–128. **[CrossRef]**

24. Baxa J, Vondrakova A, Matouskova T, et al. Dual-phase dual-energy CT in patients with lung cancer: assessment of the additional value of iodine quantification in lymph node therapy response. Eur Radiol 2014; 24:1981–1988. **[CrossRef]**